EUROPEAN ORGANIZATION FOR NUCLEAR RESEARCH
European Laboratory for Particle Physics

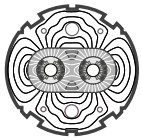

LHC Project Report 5

Large Hadron Collider Project

Adsorption Isotherms of H_2 and Mixtures of H_2, CH_4, CO and CO_2 on Copper Plated Stainless Steel at 4.2 K.

E.Wallén

Abstract

Adsorption isotherms in the pressure range 10^{-11} to 10^{-6} Torr have been measured for H_2 and mixtures of H_2 and CH_4, CO and CO_2 on copper plated stainless steel at 4.2 K. The measurements have been focused on the behaviour of the isotherms at low surface coverage, up to a few monolayers of adsorbed gas on the cold surface. The isotherms were measured in a static situation with a small amount of gas injected for each point on the isotherm. Co-adsorption measurements of H_2 with CH_4, CO and CO_2 as well as adsorption of H_2 on condensates of CH_4, CO and CO_2 have been made. A cryotrapping effect of H_2 is seen when co-adsorbing the gas mixtures, especially strong for the mixture of H_2 and CO_2. The measurements show that CO_2 condensed at 4.2 K may have a porous structure that H_2 can penetrate, while CO and CH_4 have rather dense structures when adsorbed at 4.2K. The measurements have been done within the framework of the Large Hadron Collider (LHC) project[1] at CERN, Geneva, Switzerland, where superconducting magnets will be used to produce a magnetic field of about 9 T around the arcs of the 27 km long quasi-circular accelerator. Synchrotron radiation produced by the circulating proton beam in the superconducting magnets will induce desorption of neutral gas molecules, mainly H_2, CH_4 , CO and CO_2, from the inner surface of the vacuum chamber. The desorbed gas molecules will be physisorbed on the cold surfaces in the vacuum chamber and they may induce vacuum instabilities in the accelerator. Hence it is of importance to have knowledge of the mixed adsorption isotherms of these gases at low temperatures.

LHC-VAC

Administrative Secretariat
LHC Division
CERN
CH - 1211 Geneva 23
Switzerland

Geneva, 8 March 1996

I. INTRODUCTION

A. Background

The use of superconducting magnets in accelerators has re-triggered an interest in the understanding of the physisorption process at low temperatures. Even though a large amount of work has been carried out in order to understand the physisorption process there is still no single theory that can describe its behaviour, nor with good confidence, predict the behaviour of the isotherm of a common gas like H_2 on a metal surface at low temperature. The physisorption phenomenon has experienced varying attention since it was first discovered about 100 years ago when cryogenic liquids became available. Application of the physisorption process similar to the situation in an accelerator appears in cryopumps for space simulators, fusion reactors and UHV applications to obtain efficient and contamination-free pumps. Earlier studies of the H_2 isotherms have, with a few exceptions, in principle treated either H_2 physisorption on porous media, like molecular sieve, or condensation in thick layers of adsorbed gas. The situation in the accelerator is different. The substrate is an ordinary metal surface and the interesting part of the isotherm is in general the sub monolayer part of the isotherm with a vapour pressure several orders of magnitude below the saturated vapour pressure. The presumptive problems existing in accelerators using superconducting magnets stem from the synchrotron radiation induced desorption of neutral gas molecules from the walls of the beam vacuum tube. There are already existing accelerators, for example HERA in DESY, Hamburg, Germany, which use superconducting magnets with large cold metal surfaces exposed to only small amounts of synchrotron radiation. The difference between the existing accelerators and the planned Large Hadron Collider, LHC, at CERN, Geneva, Switzerland, is that in LHC the intensity of the synchrotron radiation emitted from the beam will cause sufficient desorption of neutral gas molecules from the vacuum chamber wall to be able to lead to vacuum instabilities in the accelerator. The required beam-gas lifetime for the LHC is 100 hours. Due to nuclear scattering losses this implies a H_2 gas density $\leq 9.8\ 10^8$ molecules/cm^3, or correspondingly less for heavier gases. In the LHC there will be a need of a so-called beam screen since the cooling system producing the 1.9 K superfluid He in the superconducting magnets cannot accept the heat input of 0.4 W/m of synchrotron radiation plus the comparable lower resistive wall losses due to the beam image currents. Together these would imply a cryogenic plant 4 times the foreseen size. In the present design of the LHC the beam screen consists of a stainless steel tube with a 50 μm layer of Cu electrodeposited on the inside surface[1,2]. It is this Cu plated surface which will adsorb the synchrotron radiation and carry the beam image currents from the 7.0 TeV protons. The synchrotron radiation both desorbs gas from this surface and heats the beam screen which will be cooled to between 5 and 20 K. The dominating desorbed gases are H_2, CH_4 , CO, CO_2 and H_2O. Of these gases only H_2 has a non negligible vapour pressure at the actual temperature of the beam screen, 5 - 20 K. Since the desorption of H_2 is the most important contribution to the total gas load in the beam tube and H_2 also has the highest vapour pressure at low temperatures it is important to

know the pressure resulting from different coverages of H_2 on the beam screen surface. This article gives details of measurements of the adsorption isotherm for H_2 and mixtures of H_2 with CH_4 , CO and CO_2 at 4.2 K on a surface identical to that of the beam screen. The gas species adsorbed on the real beam screen will experience an environment very different from the calm and temperature stable surface used for this study due to exposure to disturbing synchrotron radiation together with ion and electron bombardment. However, in order to obtain a reference case for the more complicated case involving the varying temperature and synchrotron radiation it is of interest to study a simpler situation which later on will hopefully contribute to the understanding of the real situation in the LHC accelerator.

B. Physisorption

Different cases of adsorption are commonly classified into either chemisorption or physisorption. Physisorption is sometimes called cryosorption and it has to be distinguished from cryocondensation or just condensation. In condensation the adsorbate gets adsorbed on its own liquid or solid while in physisorption the adsorbate is adsorbed on a substrate which consists of a material other than the adsorbate. Physisorption is a "weak" adsorption in which the single molecule or atom binding energy is a few tens of meV and in which there is no apparent chemical bond formation. In chemisorption where the interaction results in a redistribution of charge, so the electronic or chemical structure of the adsorbing particle is significantly changed, the typical binding energy is a few eV. Physisorption leaves the electronic structure of the adsorbate essentially unchanged. Stable physisorbed species of H_2 on cold (T≈15K) surfaces of Cu have been detected[3] using high resolution electron energy loss spectroscopy (HREELS). The HREELS spectra display rotational excitations and internal H-H stretch vibrations that show only minute shifts compared to the gas phase values. This shows that the chemical state of the physisorbed molecules is virtually identical to the gas-phase state. The physisorbed molecules are trapped in a potential well formed by a long range attractive force and a short range repulsive force between the molecules and the surface[4]. The long range attractive force is due to van der Waals interaction. The attraction stems from coupling between the dipole fluctuations in the adsorbate and the substrate and it varies asymptotically as z^{-3}, where z is the distance from the substrate. The repulsion for small z sets in when the electron cloud of the adsorbate starts to overlap appreciably with the electrons of the solid substrate. The repulsive part is related to the charge density of the solid substrate and for metals it grows exponentially with decreasing z. In comparison with the attractive part, the repulsive potential is very steep and in some cases it is approximated by an infinitely hard wall. A realistic modelling of the interaction is [5,6]

$$V_0(z) = V_0 \exp(-\alpha z) - \frac{C_{vdW}}{(z - z_{vdW})^3} f\left(k_c (z - z_{vdW})\right), \quad (1)$$

which contains an exponential repulsive part and a long range z^{-3} attractive part. The parameters z_{vdW}, k_c and the function f in the attractive part are related to complications in the description of the van der Waals interaction. V_0 is a repulsive potential parameter and α is the repulsive exponent. Jellium calculations[7] have shown that with z representing the distance from the first plane of atoms in the substrate, the z^{-3} dependence should be replaced by a $(z-z_{vdW})^{-3}$ dependence since the effective location of the image plane differs from the plane of the first atoms in the solid. k_c is a cut-off parameter and in combination with the function $f(x)=1-[2x(1+x)+1]e^{-2x}$ it describes the saturation of the van der Waals attraction due to the finite size of the molecule. C_{vdW} is the van der Waals constant which gives the strength of the attractive force. The strength of the van der Waals attraction is related to the polarizability of the adsorbate as well as the ability of the substrate to image the fluctuating dipoles of the adsorbate. Metal substrates have an incomplete screening of the high frequency components of the fluctuating dipole field. The description of the physisorption interaction has so far been one-dimensional and the surface of the substrate treated as smooth and without structure.

In a detailed treatment of the physisorption process the corrugation of the surface due to the atomic crystal structure of the substrate has to be taken into account. The long range attractive force shows little variation with corrugation while the short range repulsive force depends strongly on the corrugation of the surface[8]. Insulators are considered as strongly corrugated, whereas the conducting electrons of metals fill the gap between the atoms and make the surface rather smooth. For many systems, like H_2 interacting with a close-packed noble metal surface, the corrugation is very small and the one-dimensional representation is sufficient for most applications. For a technical surface, like an electrodeposited Cu surface, the crystal structure as well as the purity and oxidation of the surface are not known, which limits the description of the physisorption interaction to an in principle qualitative picture.

Information about the corrugation of the substrate and the attractive van der Waals force between the adsorbate and the substrate can be derived from scattering experiments where a well-defined beam of adsorbate atoms or molecules are scattered from a well-defined crystal face of the substrate. Detailed studies of the H_2-Cu interaction have been carried out by, among others, ref.[9],[10],[11],[12]. The depth of the physisorption well for the H_2-Cu interaction is commonly believed to be 22 meV[11] but more recent measurements have shown a substantially higher value of 31 meV[13]. Even if the well depth is rather large, the molecules trapped in the physisorption well are less tightly bound than the well depth might indicate. The molecules are trapped in a number of allowed bound-state levels with bound-states energies lower than the well depth. The lowest bound state of H_2 on Cu has an energy of 25.5 meV. An incident molecule will be influenced by the potential and accelerate towards the surface but as long as it does not change its total energy it will simply bounce off the surface out of the well and escape back into vacuum. To stick and become adsorbed the

molecule must experience some friction, i.e. give up energy to the substrate or internal modes such as rotations or vibrations[14,15].

Physisorption, which does not involve any change in chemical configuration, is very inefficient in adsorbing the kinetic energy of incident particles. The probability for sticking of an incident H_2 molecule with a kinetic energy of about 20 meV on a bare metal surface is of the order of a few percent. Physisorbed H_2 molecules are not tightly bound in localised sites and their freedom to translate parallel to the surface when struck by an incident particle provides an efficient means for absorption of a substantial amount of the incident kinetic energy. In fact, the sticking of H_2 on Cu is dominated by particle-particle collisions and the probability of sticking increases with the number of molecules already adsorbed on the surface. For a relative surface coverage θ equal to zero the probability of sticking is about 0.1 for H_2 molecules with 15 meV of kinetic energy and it increases linearly with θ up to $\theta = 1$ where it is close to unity[10]. The increase in sticking coefficient with θ in physisorption of H_2 on Cu is fundamentally different from the case of chemisorption. In chemisorption, where the pre-adsorbed species tend to block the chemisorption process, the sticking probability falls with increasing θ. The physisorbed molecules are affected by the presence of other physisorbed molecules, usually in the form of an increased binding energy with increasing θ. On the other hand, adsorption sites with high adsorption energy will be occupied earlier than less attractive adsorption sites, which might balance the increased binding energy with increasing θ caused by lateral interactions between the physisorbed molecules. For the case of the H_2-Cu interaction the difference between different adsorption sites is small compared to the forces introduced by the presence of other adsorbed molecules. The physisorbed molecule retains its identity in the condensed phase and the pair potential which determines properties of the dilute gas phase is supplemented by many-body interactions and substrate-mediated energies in the total potential energy of the dense adsorbed phase[4].

In the case of gas physisorbed on metals, the growth of the adsorbed gas layer is a combination of layer and island growth. After forming the first monolayer, or a few monolayers, the subsequent layer growth is thermodynamically unfavourable, and islands are formed on top of the intermediate monolayers[16]. The lateral interaction between the adsorbed molecules and the substrate is very complex, especially if there are more than one type of adsorbed molecule on the substrate, and in many applications it is more feasible to have an experimental/empirical approach to the physisorption interaction which leads to the aim of this study - to measure adsorption isotherms of pure and mixed H_2 at low temperatures and compare the results with existing models of adsorption isotherms for physisorption.

C. Isotherms

Although physisorption has been studied extensively for many years, it is still not completely understood and no single theory can accurately describe this phenomenon. There are, however, a number of theories for adsorption

isotherms which have survived over the years and the most frequently appearing equations are described below. P is the equilibrium pressure at surface coverage S.

The simplest adsorption isotherm, often called Henry's law[17],

$$S = c\,P, \qquad (2)$$

where c is a temperature, adsorbate and substrate dependent constant, in which the amount of adsorbed gas varies linearly with the pressure originates from observations of the solubility of gases in liquids and it builds on the assumptions that both the gas and the adsorbed phase are dilute enough to obey the perfect gas law and that there are no lateral interaction between the adsorbed gas molecules[18]. When plotted on a log-log chart Henry's law represents a straight line with unit slope. Henry's law is the expected behaviour for all physisorption isotherms at very low surface coverage, up to some fraction of a percent of a monolayer; however, the true range of applicability of Henry's law is very short. In fact it is often below the range of experimental accessibility.

Another isotherm is the Freundlich equation[19], which in principle only has empirical justification

$$S = c\,P^{1/n} \qquad (3)$$

Where c and n are temperature, adsorbate and substrate dependent constants. When S is plotted against P on a log-log chart the Freundlich isotherm is represented by straight line with slope 1/n. In all cases n is greater or equal to unity[20]. A large number of experimental isotherms have shown to obey the Freundlich equation but an even larger number cannot be described by this equation.

The Langmuir isotherm is another isotherm that occupies a central position in the field of adsorption[21]. It originates from one of the first theoretical treatments of adsorption. It is based on the assumptions that the substrate has only energetically equal adsorption sites and that there is no lateral interaction between adsorbed molecules. It is further assumed that it is not possible for the adsorbed molecules to move between different sites via surface diffusion and that adsorbate molecules that impinge on a bare surface have a certain probability of being adsorbed, but those impinging on a site already occupied by an adsorbed molecule would be immediately re-evaporated, thus the Langmuir model is limited to monolayer coverage. The isotherm resulting from the assumptions above can be written as

$$S = \frac{S_m bP}{1 + bP} \qquad (4)$$

In practice both S_m and b are determined from experiments but they have well defined physical significance. S_m is the monolayer capacity and b is an adsorption coefficient given by

$$b = \frac{\alpha_0 \exp(\Delta H_a / kT)}{\beta_0 (2\pi m kT)^{1/2}} \qquad (5)$$

where α_0 and β_0 are the condensation and evaporation coefficients, m is the mass of the adsorbent molecule, ΔH_a is the adsorption energy k is Boltzmann's constant and T is the absolute temperature. A linear plot of the isotherm data in P/S and P coordinates would provide a straight line with an intercept of $1/S_m b$ and a slope of $1/S_m$. The Langmuir isotherm is in general more applicable to chemisorption than physisorption and it has been shown to be successful in describing the isotherm of molecular hydrogen on metal surfaces at temperatures much higher than the temperatures for physisorption, while for physisorption of H_2 on Pyrex glass[22], porous materials like silicagel[23] and gas condensates[24,25] at low temperatures and pressures it fails.

With the adsorption theory from Brunauer, Emmet and Teller[26,27], hereinafter referred to as BET, the assumptions of the Langmuir theory are expanded into the multilayer region. The basic assumption of the BET theory in its simplest form is that molecules in the first layer can serve as adsorption sites for molecules in the second layer and so on. The adsorption or desorption will always take place in the topmost layer and for the exchange of molecules between the lower layers a dynamic equilibrium is assumed. It is further assumed that the first layer will have some value for the heat of adsorption, ΔH_a, but for all succeeding layers, the adsorption energy is assumed equal to the heat of vaporisation of the pure bulk adsorbate, ΔH_L. The assumption of the BET theory leads to the BET isotherm for multi-monolayer adsorption on a free surface which has the form

$$S = \frac{S_m \alpha P}{(P_0 - P)(1 + (\alpha - 1) P/P_0)} \qquad (6)$$

where S_m is the monolayer capacity, P_0 is the saturated vapour pressure and α is a dimensionless parameter approximately equal to $\exp((\Delta H_a - \Delta H_L)/kT$. For any particular surface the values of S_m and α have to be determined from the measured adsorption isotherms. The BET equation may be transformed into,

$$\frac{P}{S(P_0 - P)} = \frac{1}{\alpha S_m} + \frac{(\alpha - 1)}{\alpha S_m} \frac{P}{P_0} \qquad (7)$$

which would yield a straight line for the expression $[P/S(P_0-P)]$ plotted versus P/P_0. The intercept is $1/(S_m\alpha)$ and the slope is $(\alpha-1)/(S_m\alpha)$. Since α in general is large for the case of physisorption, the slope is close to $1/S_m$.

These attempts to predict the shape of an isotherm from a few basic assumptions have had limited success in describing the real situation, not least due to crude assumptions. An interesting theory, which does not try to predict the shape of the isotherm, is the potential theory, developed by Polanyi[28]. This theory assumes that a potential field exists near the substrate surface and the adsorbate molecules are bound to it like an atmosphere is bound to a planet. The adsorbing molecules are treated as being more compressed close to the substrate and their density decreases outward. The adsorption potential at a point near the substrate is defined as the work done by adsorption forces in bringing in molecules from the gas phase to that point. The adsorption potential, $\varepsilon = f(\phi)$, is a function of ϕ, which represents the adsorbate surface coverage S divided by δ_T, the liquid density of the adsorbate at the temperature T. The function $\varepsilon = f(\phi)$ decreases from its maximum value at $\phi = 0$, (S = 0), to its minimum value when the saturated vapour pressure is reached at ϕ_{max}, ($S = S_m$). It should be noted that the interpretation of S_m is not the same in this theory as in the BET theory. The function $\varepsilon = f(\phi)$ is called the characteristic curve and it is postulated to be independent of temperature. The adsorption potential ε_i at $\phi_i = S_i / \delta_T$ is given by the energy needed to compress the vapour from the equilibrium pressure P_i to the saturated vapour pressure P_0.

$$\varepsilon_i = k\,T \ln(P_0/P_i) \qquad (8)$$

From one measured isotherm it is possible to predict the isotherm for different temperatures at the same ϕ as measured but there is no prediction for other ϕ. An important assumption in the potential theory as described above is that the adsorption temperature is well below the critical temperature of the adsorbate gas. The characteristic curve has proved to be very successful in predicting the temperature dependence of physisorption. Experimental work done by Dubinin and Radushkevich[29] has shown that the low pressure adsorption isotherms for many adsorbate-substrate combinations can often be described by the function

$$\ln(S) = \ln(\phi_{max}\,\delta_T) - D\,\varepsilon^2 \qquad (9)$$

called the DR equation. D is an adsorbate-substrate dependent constant to be fitted with experiment. Discrepancies can be seen in the high pressure end, close to the saturated vapour pressure and in the low pressure end where the isotherm approaches Henry's law. If the temperature dependence of the density of the liquid adsorbate is assumed to be negligible it is possible, as shown by Kaganer[30], to use the DR equation to estimate the monolayer capacity of the substrate. In combination with (8) we arrive at the famous DRK equation which is

$$\ln(S) = \ln(S_m) - D\,(kT \ln(P_0/P))^2 \qquad (10)$$

where P is the equilibrium pressure at surface coverage S, and S_m can be seen as the monolayer capacity of the surface. The difference between (9) and (10) is that in (9) the maximal volume ϕ_{max} is fixed, thus giving a small variation

of the amount of molecules in this volume with the temperature dependence of the density of the liquid adsorbate. In (10) the density variation with temperature is neglected and this gives a constant amount of molecules in ϕ_{max} , an amount which is interpreted as the monolayer capacity. The DRK equation has in many cases been able to describe the isotherms for porous substrates and condensed gas substrates as well as very low pressure isotherms for metal and glass substrates, situations where the BET and other theories have failed.

Comparative studies by Hobson[31] of the monolayer capacity given by the DRK equation compared to that given by the BET equation have shown that the DRK equation in general gives lower values for the monolayer capacity than the BET equation. The BET equation usually describes an isotherm well in the region $0.003< P/P_0<0.3$ while the DRK equation is valid at lower pressures. Hobson suggests that the DRK monolayer coverage is the greatest coverage for which the lateral adsorbate-adsorbate interactions can be neglected.

D. Cryotrapping

A gas like H_2 is weakly physisorbed on a cold surface even at low temperatures and it is often the only gas which can be detected by the instruments in a cryopumped vacuum system, since the vapour pressure of the other gases is negligible at 5-20 K. Even if the other gases desorbed by the synchrotron radiation induced desorption cannot be seen by the instruments i.e. they do not remain in the gas phase, they will still be present on the substrate surface. It is not pure H_2, but a mixture of H_2 and the other gases, which will be physisorbed on the cold surface. If such a gas mixture physisorbs on a cold substrate, the gas with weak physisorption may be incorporated into the condensate of the other gases which are more strongly physisorbed, and, provided the weakly physisorbing gas is not too dominant in the mixture, its vapour pressure will be suppressed compared to the case of physisorption of the pure gas. The effect of pressure reduction of the gas with weak physisorption when it is coadsorbed simultaneously with other, more strongly, physisorbed gases is called cryotrapping.

Cryotrapping may be regarded as a special case of physisorption taking place on a continuously self-renewing substrate surface. The efficiency of the pressure reduction by cryotrapping strongly depends on the gas used as partner to the weakly physisorbed gas[32]. Ar, NH_3 and CO_2 have been shown to be efficient in the cryotrapping of H_2 while CO and especially CH_4 have a more moderate influence on the vapour pressure of H_2. The weakly physisorbed molecules are believed to become trapped inside the crystals of the partner gas as well as being adsorbed on the outside of the crystallite grains. Wandelburg[33] has suggested that, in the H_2/Ar case, clusters or islands of H_2 form within the condensate of Ar. Hengevoss and Trendelburg[34] have shown that the trapping ratio, which is the number of partner Ar molecules needed to trap a H_2 molecule, rises exponentially with temperature. Schimpke and Schugerl[35] who examined the cryotrapping of H_2 by Ar and CO at 4.2 K found that one Ar atom was capable of trapping

two H_2 molecules while two CO molecules were needed to trap one H_2 molecule. They also make the conclusion that the polarity of the trapping gases has no influence on their efficiency in the cryotrapping process and suggests that it is rather the sticking coefficient of the trapping gas which determines the efficiency.

The cryotrapping phenomenon has found applications in cryopumps where an additional gas, for example CO_2, is admitted into the pump in order to enhance the pumping of H_2 and He, gases which normally have a high saturated vapour pressure at the temperature of the cryopump. In this case, where the adsorbed gas layers are very thin, up to a few monolayers, it is a different situation than the one explored in earlier studies of cryotrapping which treats thick layers of adsorbed gas and also treats higher pressures in dynamic situations instead of as here a static situation at pressures in the UHV range.

E. Physisorption on gas condensates

When the substrate has become covered with a certain amount of adsorbate molecules, the saturated vapour pressure is reached. In general the saturated vapour pressure is too high to be accepted and the substrate has to be reconditioned, i.e warmed up and recooled before a sufficiently low pressure can be obtained again. In cryopumps, which usually have the design aspect of high pumping capacity between reconditioning warm-ups, the substrate is, in general, chosen to consist of materials with large adsorption capacity. Such materials are porous solid substrates, such as molecular sieves[36] and activated charcoal[37], but also condensates of gas with a considerably higher melting point than the adsorbate[38]. By condensation of gases, such as CO_2, polycrystalline porous adsorbents with a clean surface can be produced.

Many measurements of the He and H_2 physisorption capacity of CO_2 and Ar have been carried out due to the interest in practical applications in cryopumps. The DRK equation (10) has shown to be the isotherm which best describes the physisorption on gas condensates[24,25,38,39]. The isotherm for physisorption on gas condensates, as well as on porous substrates, does, in general, show a very low, often undetectable pressure for small amounts of physisorbed adsorbate and the pressure slowly increases until the substrate gas condensate is saturated with adsorbate and a very steep pressure rise up to the saturated vapour pressure takes place.

Thorough investigations of different gases used as the substrate condensate have been carried out. In general, CO_2 is considered to be an efficient gas as the condensed substrate, while CH_4 is less efficient. The situation for CO is not known. The H_2 adsorption capacity of a CO_2 condensate depends on the temperature at which it was formed[39], at what rate it was created[24], its temperature history and presence of other gases during the formation[40]. The H_2 pumping speed of a CO_2 condensate in the temperature region 6-11 K increases with temperature[41] which indicates that the determining process for the rate of the pumping speed is diffusion of H_2 into the CO_2 condensate. During the deposition of the CO_2 condensate thermal spikes, which reduce

the adsorption capacity, can appear if the temperature of formation T_f is less than 8 K[42]. The thermal spikes stem from an unstable structure of the CO_2 condensate formed at $T_f < 8$ K. Not only is the adsorption capacity larger before the thermal spike than after but sometimes, if the CO_2 condensate already contains adsorbate gas, a resulting sudden pressure peak of adsorbate gas is seen simultaneously with the thermal spike. There is a maximum for the H_2 adsorption capacity of the CO_2 condensate of about one H_2 molecule to three CO_2 molecules. The DRK monolayer capacity for a CO_2 condensate formed at 4.2 K is about 0.073 ($molH_2/molCO_2$)[39] and for a CH_4 condensate formed at 4.2 K about 0.040 ($molH_2/molCH_4$)[25]. The adsorption capacity value for the H_2-CO_2 combination might be questionable, since, at temperatures lower than about 10 K, it has proved difficult to obtain a true equilibrium pressure for the H_2-CO_2 combination, which probably is correlated to the diffusion process of H_2 into the condensate, which is suppressed at low temperatures. Other measurements[43], unfortunately not described in the DRK formalism, indicate a higher value. For the CH_4-H_2 combination at temperatures above 4 K there are no obstacles to obtain an equilibrium situation and the adsorption capacity of CH_4 has not been shown to depend on the temperature at which it was formed.

F. The structure of solid H_2, CH_4, CO and CO_2

Solid H_2 formed at 4.2 K has an f.c.c. structure with a nearest neighbour distance of 0.395 n m[44]. Solid H_2 has two different crystal structures. If the condensate is formed at a temperature higher than 5.3 K, it has a h.c.p. structure and if the condensate is formed at temperatures lower than 5.3 K it has an f.c.c structure[33]. The nearest neighbour distance is the same for both crystal structures. The different structures have different saturated vapour pressures with about 5 times lower pressure for the h.c.p. phase than predicted by the temperature dependence of the saturated vapour pressure of the f.c.c phase. The heat of vapourisation remains the same. There is a hysteresis in the saturated vapour pressure when passing the 4-5 K region which originates from a mutual transformation. The transformation process is rather slow with a time scale of hours. Solid CO_2 has an f.c.c. structure structure with a nearest neighbour distance of 0.40 n m[45] and the crystallite size differs with the temperature of condensation and the conditions during the formation of the condensate. In general the crystallite size gets smaller with decreasing temperature at condensation and it has a minimum crystallite size of about 10 n m[46] when the temperature of condensation is 10-20 K. The crystallite size for temperatures below 10 K is perhaps even smaller but, the condensates formed at such low temperatures are not stable and thermal spikes due to rearrangements in the condensate are seen during the deposition of the condensate[47]. Solid CH_4 formed at 4.2 K has an f.c.c. structure with a nearest neighbour distance of 0.41 n m[48,49] and a crystallite size of 10 nm[50]. At temperatures lower than 60 K CO has, a f.c.c structure with an nearest neighbour distance of 0.398 nm[51].

The literature cited is not claimed to be a complete bibliography of the subject but it may make the field more accessible to the interested reader.

II. EXPERIMENT

The experimental set-up can be seen in fig.1. The 100 μm thick electroplated copper coating is on the inside of a stainless steel cylinder, length 71 cm and Ø 10 cm (The choice of 100 μm thickness of the Cu layer originates from an earlier design of the beam screen, in the present design[2] the thickness is 50 μm). The bottom and the top of the cylinder are not Cu plated but have a stainless steel surface which results in a 92% coverage of Cu on the stainless steel surface. The fact that not 100% of the surface is Cu plated is neglected in this case and surface coverages are calculated by dividing the total number of molecules with the total cold surface, 2375 cm^2, including the top and bottom parts. The total volume of the system is 9.04 l, where the cold part represents 61% of the total volume. The cylinder is immersed in a bath of liquid He in a standard glass cryostat with an intermediate temperature barrier of liquid nitrogen. The He bath is slightly over pressurised, 30 mbar over atmospheric pressure. Since the atmospheric pressure is not constant with time there is a small variation in the temperature of the He bath, which is visible in variations of the saturated vapour pressure of H_2 in the experiments. Considering the large pressure range of the measurements this is negligible. The cylinder is connected to the measuring instruments, a Bayert-Alpert ionisation gauge and a quadrupole residual gas analyser, at room temperature via a 50 cm long Ø 31.5 mm stainless steel pipe. In the pipe there are Cu discs which absorb the room temperature heat radiation from the upper part of the system. Gas is injected into the system via a leak valve and from a known control volume with an absolute pressure manometer.

When doing co-adsorption of different gases, all gases to be coadsorbed are put into the control volume and let through the same leak valve into the cold part of the system. The gas is let into the system through an injection line with small holes lateral along its length which hangs into the cold part of the system, giving a quasi uniform distribution of the injected gas on the cold surface. Experience from early measurements with the system has shown the necessity of having a distributed injection of the gas to be adsorbed. If the injected gas is not evenly distributed over the cold surface, local surface concentrations of the adsorbed gas appear, which give rise to a too high measured pressure and irreproducibility of the measurements.

The ratio of the gases that pass the leak valve is different from the ratio in the control volume. It might be expected that the leak rate through the leak valve for different gases would differ as the square root of the mass ratio between the gases; this is however not true and there are less molcules with low mass than expected. A phenomenom which might depend on local drainage of molecules with low mass close to the leak valve. In order to know the composition of the gas passing the leak valve a calibration procedure was made. Individual pure gases were injected into the system to calibrate the residual gas analyser. Using this calibration, the composition of the gas mixture passing the leak valve was determined.

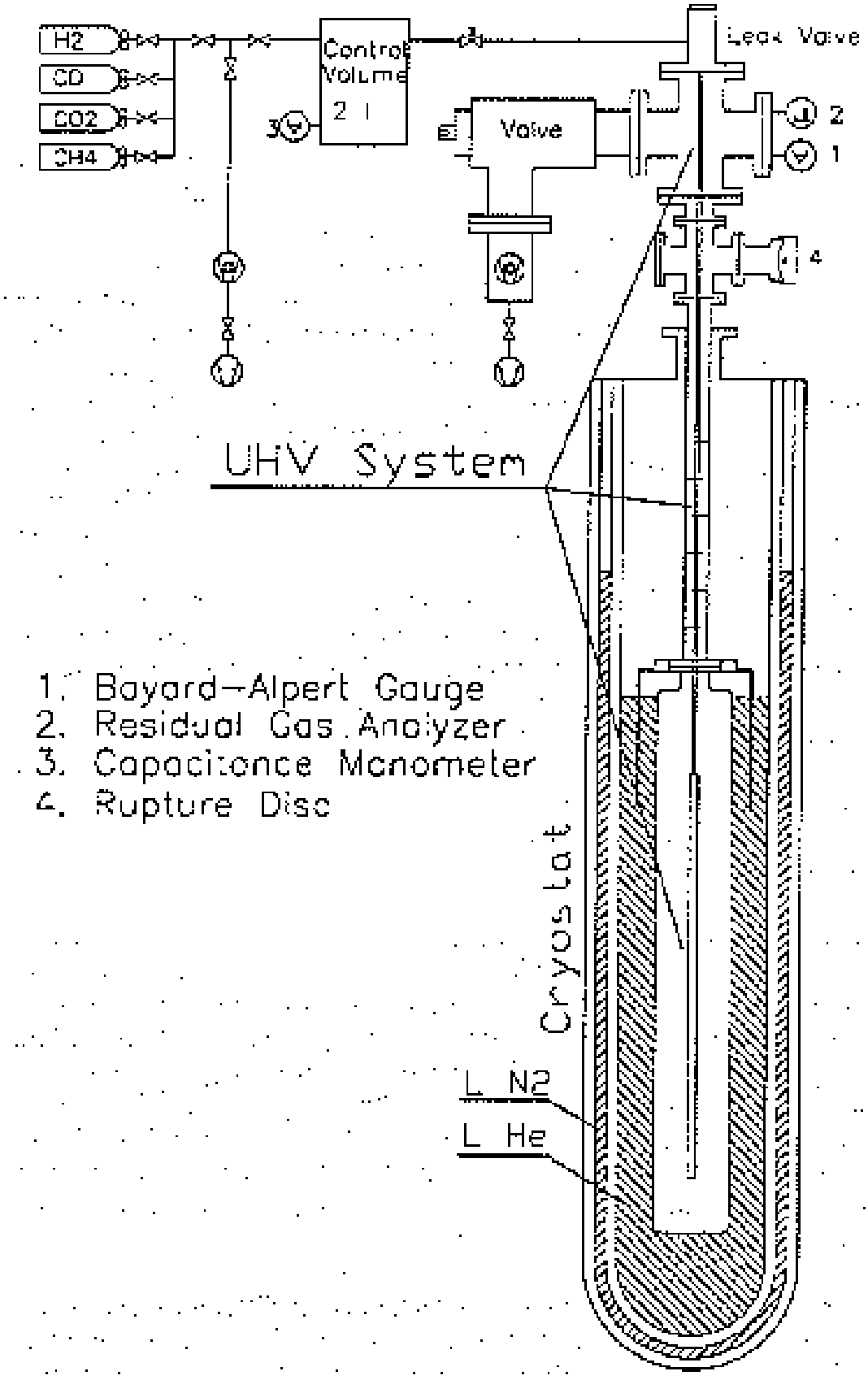

Fig.1 Experimental setup. The cryostat, about 1.2 m high, is a standard glass cryostat with an intermediate temperature barrier of liquid N_2. There is a perforated injection line for the injected gas that hangs down into the cold part of the UHV system. The injection line leads the injected gas directly into the cold part of the UHV system

The temperature of the injection line is, by conduction from the warm end, around 130K. When making the injection of gas mixtures containing CO_2 the injection pipe is heated up to more than 200 K. The physisorption properties of a cold surface can be affected by heat radiation coming in from warm parts of the vacuum system as shown by Lee[52] and Benvenuti et al[53]. Such effects are neglected in this set-up since the temperature of the injection line, which is the only possible heat source in the cold volume, is rather low and the solid angle with this temperature seen from the cold wall is small.

There is a copper shield mounted at the top of the cold bottle. The copper shield has a thermal conductivity that is very large compared to the stainless steel bottle and pipe which gives a constant temperature for the top flange as long as some part of the copper shield is still in the He bath. This gives a stable temperature for about 8 hours which is sufficient to measure a complete adsorption isotherm.

Between each measurement, the top of the system was baked-out for 24 hours at 250 °C and the lower part was heated up to about 90 °C for at least 24 hours. It is believed that the "soft" bake-out of the Cu plated stainless steel surface gives a clean surface without going to the extreme where adsorption sites with a very high adsorption energy become free. The background pressure in the system just before starting a run is typically 2.0 10^{-10} Torr, N_2 equivalent at 298 K, with the bottle at 4.2K and the turbomolecular pump valved off. The background pressure is dominated by H_2 to about 90%. A stable background pressure is reached first several hours after the cryostat is filled with liquid He and the turbo pump is valved off. The isotherms were measured in a static situation by injecting a small amount of gas and waiting for the pressure to become stable. The time to reach a stable pressure at low coverage is typically 20 minutes. At high coverage the time to reach a stable pressure is reduced to a few minutes. The background pressure is subtracted from the measured pressure. In order to avoid that fluctuations in the background pressure are interpreted as changes in the equilibrium pressure in the cold volume, points representing a pressure rise of less than about 10% over the background pressure are not taken into account. This gives a low pressure limit of the measurements of about 2.0 10^{-11} Torr, N_2 equivalent at 298 K. Measurements with the RGA have shown that for all injected gas mixtures only the H_2 pressure is visible at the top of the system. All the other gases have too low a vapour pressure at 4.2 K to be detected.

Thermal transpiration effects were taken account for by applying the Knudsen relationship between the gas density in the cold lower part of the system and the top part, which is at ambient temperature. The Knudsen relation states[54] that if the pressure P_A in a cold vacuum vessel at temperature T_A is measured with a gauge, at room temperature T_B , connected to the cold vacuum vessel the reading P_B of the gauge has to be compensated for the temperature difference between the two volumes. When the gas density is sufficiently low that the flow is molecular, the following Knudsen relation holds for pressure $P_A = (T_A/T_B)^{1/2} P_B$ and for the gas densities n_A and n_B the relation is inversed $n_A = (T_B/T_A)^{1/2} n_B$. The

Knudsen relationship is valid at low pressures for an aperture-like connection between two volumes of different temperature and there must not be a net flow of gas between the two volumes. When the connection between the volumes consists of a tube, the Knudsen relation might be unreliable since the probability for a molecule to traverse from the hot to the cold end of the tube is greater than in the opposite direction[55]; however the Knudsen relation is generally accepted and in these measurements believed to be applicable due to the low pressure and the relatively small aperture of the pipe connecting the two volumes of different temperature.

The pressure gauge has been calibrated for H_2 and He and it is accurate to better than 10%. Instead of pressure, which represents a force per unit area, the volume density is used in this report to represent the measured adsorption isotherms. From an accelerator vacuum point of view, where the beam lifetime is affected by scattering of the circulating particles on residual gas molecules in the vacuum chamber, the density of the residual gas molecules is of interest and not the pressure they exert on the vacuum chamber walls. The gas density n is related to the pressure P via $n = 9.656\ 10^{18}$ (P/T) molecules/cm^3 with P in Torr and T in K.

III. RESULTS

All of the isotherms measured are from the same surface, a Cu plated stainless steel surface. The surface was kept at the same temperature, 4.2 K, for all measurements, except one Xe isotherm, by a boiling He bath as shown in fig.1. The Xe isotherm was measured at 77K and in this run the liquid He was replaced by liquid N_2. The surface coverage in molecules/cm^2 is represented by S.

A. The H_2 Isotherm

The measured H_2 adsorption isotherm on Cu plated stainless steel at 4.2 K is shown in fig.2. At S lower than $8\ 10^{14}$ H_2/cm^2, no pressure rise is detected at the top of the system. At $S=1.3\ 10^{15}$ H_2/cm^2 the low pressure detection limit of the system, $2.0\ 10^{-11}$ torr N_2 equivalent at 298 K, is passed and there is a moderate pressure rise with S up to $S = 1.65\ 10^{15}$ H_2/cm^2 where a very steep pressure rise with increasing S takes place and continues up to $S = 3.3\ 10^{15}$ H_2/cm^2 above which there is a distinct saturation of the vapour pressure. It is important to notice that the saturation takes place at an S equal to twice the coverage where the very steep pressure rise starts. For S larger than $5.0\ 10^{15}$ H_2/cm^2, a modest pressure decrease of about 10% has been seen. The pressure decrease has not been satisfactorily reproducible and it has been difficult to establish a better value for both the magnitude of the decrease and where it starts.

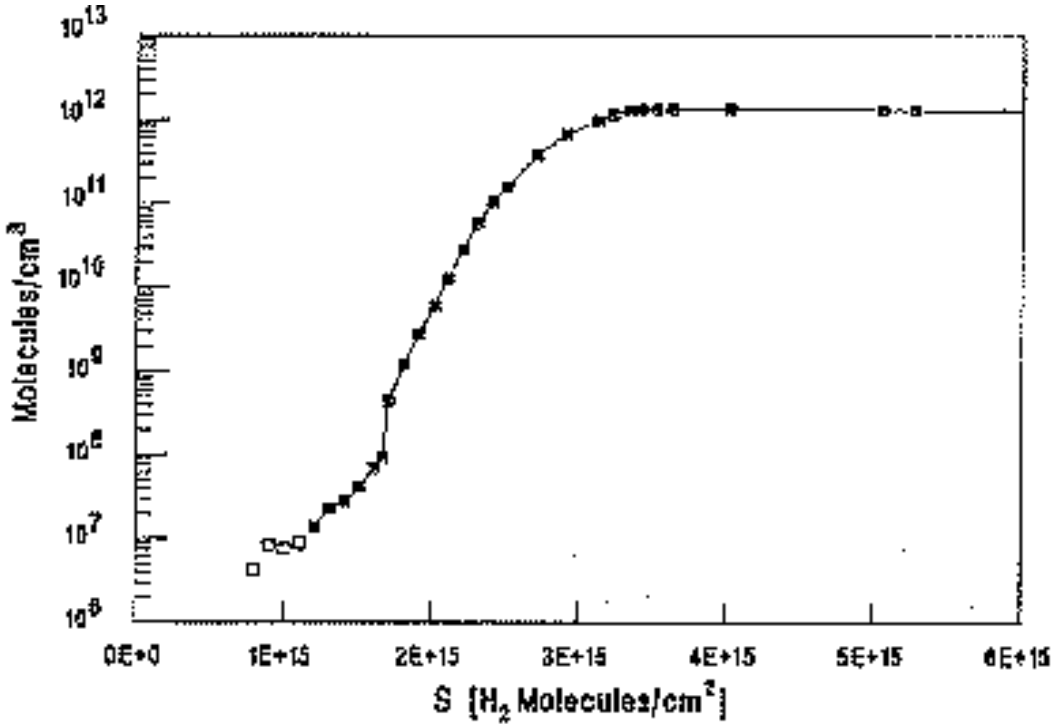

Fig.2 Isotherm for H_2 on Cu plated stainless steel at 4.2K plotted as a function of the surface density of H_2. The non filled markers represent measured points on the isotherm which are less than 10% above the background pressure at the instruments

There is an interesting difference between values of S higher and lower than $S = 1.65\ 10^{15}\ H_2/cm^2$. For S lower than $1.65\ 10^{15}\ H_2/cm^2$ the pressure is higher during injection of the gas than the equilibrium pressure reached about 20 minutes after making the injection. This difference from the equilibrium pressure decreases with S and for values larger than $1.65\ 10^{15}\ H_2/cm^2$ the equilibrium pressure is higher than the pressure during the injection. Also in the former case there is an immediate pressure rise when making the injection but, in the latter, the pressure rise is not immediate but it takes some time (~20 s) before an effect of the gas injection is seen. This observation may be interpeted as the sticking coefficient for the H_2 impigning on the Cu surface increases with S. It is however not possible with this experimental set-up to quantitatively measure the sticking coefficient for the H_2 impigning on the cold surface because of the anisotropic pressure distribution in the cold volume during the gas injection.

B. Adsorption of H_2 on gas condensates of CO, CH_4 and CO_2

Two adsorption isotherms of H_2 on precondensed layers of CO have been measured. The CO was injected just after the cryostat has been filled with liquid He and there was no rise in the pressure of CO in the warm part of the system during the injection. The rate of deposition of the precondensed CO layer was about $2\ 10^{14}\ CO/cm^2/s$. The condensate was left for about 3 hours until a stable background pressure was reached and the measurement could start. The measurements were made as described previously with a small

injection of H_2 and about 20 minutes later, when a stable pressure was reached, the pressure was noted before the next injection. The adsorption isotherms of H_2 on a precondensed layer of 1.0 10^{16} CO/cm^2 and 2.0 10^{16} CO/cm^2 as well as the isotherm of H_2 on the clean Cu surface can be seen in fig.3a.

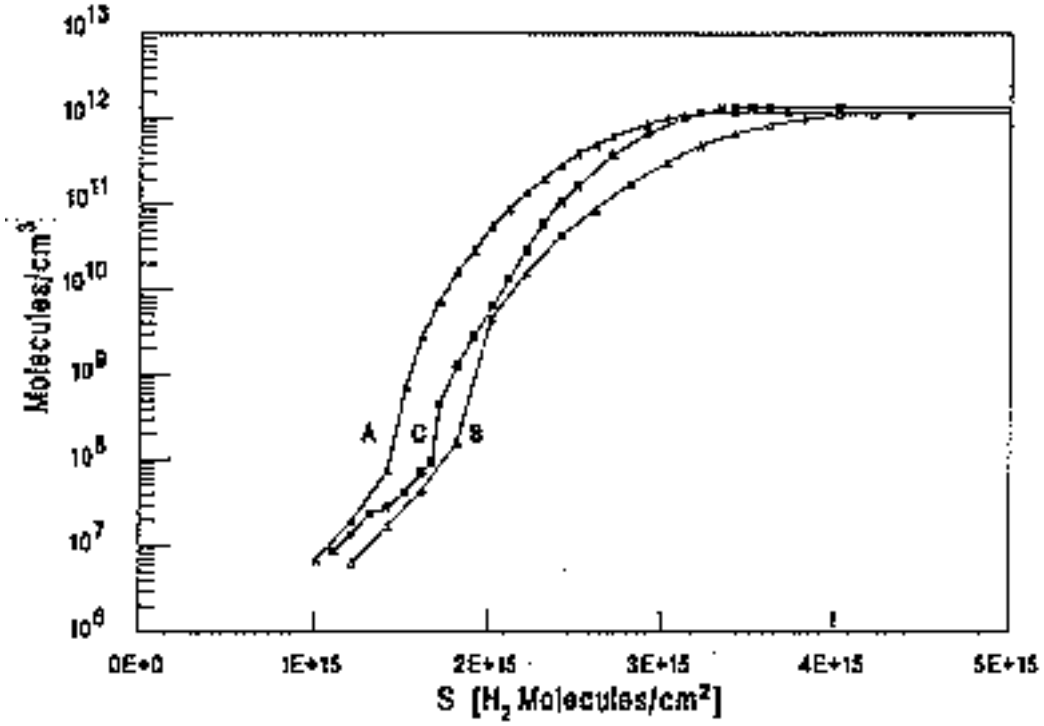

Fig.3a Isotherms of H_2 on precondensed layers of 1.0 10^{16} (curve A) and 2.0 10^{16} CO/cm^2 (curve B) and of H_2 on Cu plated stainless steel (curve C) at 4.2 K.

A surface coverage of 1.0 10^{16} CO/cm^2 represents roughly 6 monolayers of CO on the Cu surface and the isotherms show that there is no large difference in adsorbing H_2 on a gas condensate of CO compared to the metal surface. The adsorption capacity for binding H_2 before the steep pressure rise takes place has even decreased slightly with a precondensed layer of 1.0 10^{16} CO/cm^2 compared to the clean Cu surface.

Two adsorption isotherms of H_2 on a precondensed layer of CH_4 have also been measured in the same way as for precondensed CO. The adsorption isotherms of H_2 on a precondensed layer of 1.0 10^{16} CH_4/cm^2 and 2.0 10^{16} CH_4/cm^2 as well as the isotherm of H_2 on the clean Cu surface are plotted in fig.3b. There is no large effect on the H_2 isotherm with the precondensed CH_4 present on the surface. The measured H_2 isotherms on gas condensates of CH_4 have a shape similar to the measured isotherms for H_2 on gas condensates of CO. This is surprising since there is a difference in the cryotrapping efficiency for CO and CH_4. In the same way, as for precondensed CO, a layer of 1.0 10^{16} CH_4 molecules/cm^2 has less adsorption capacity than a clean Cu surface while the double surface concentration of precondensed CH_4 gives an increase in the adsorption capacity.

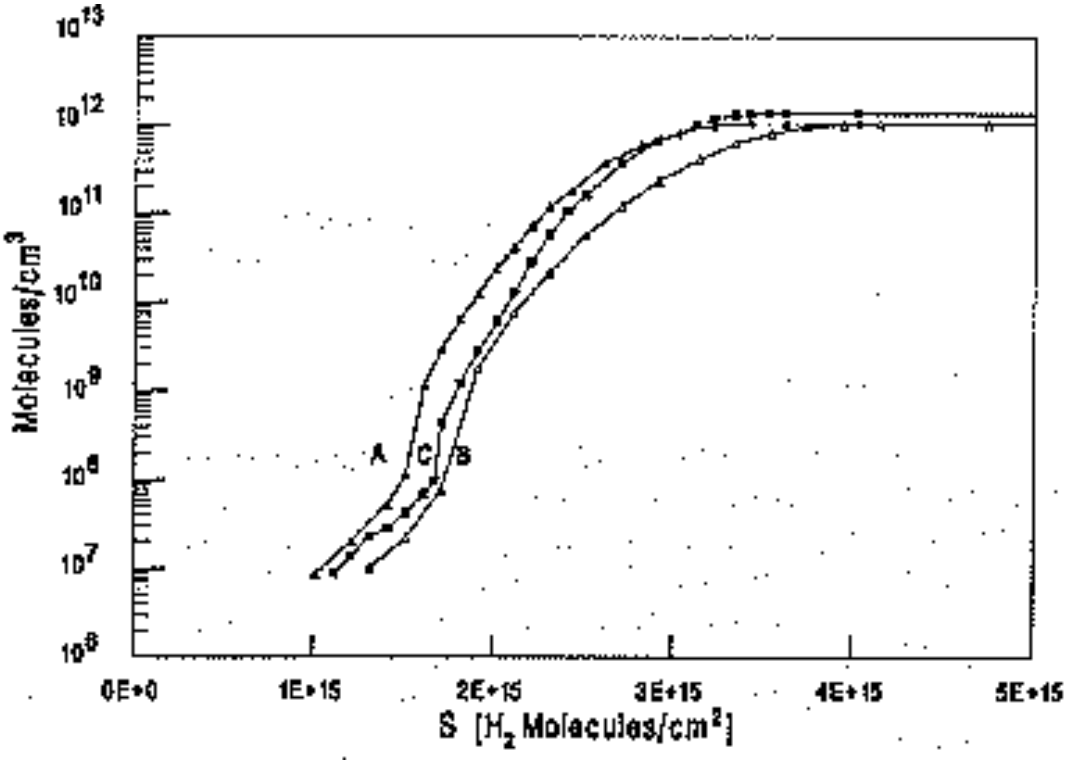

Fig.3b Isotherms of H_2 on precondensed layers of 1.0 10^{16} (curve A) and 2.0 10^{16} CH_4/cm^2 (curve B) and of H_2 on Cu plated stainless steel (curve C) at 4.2 K.

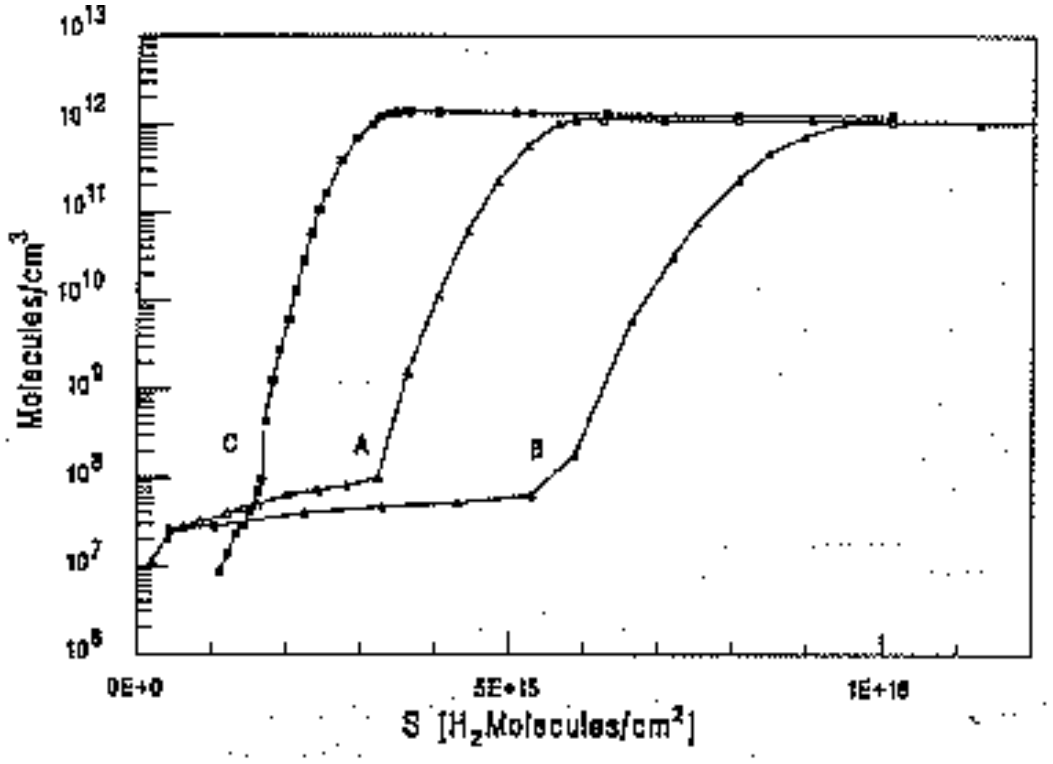

Fig.3c Isotherms of H_2 on precondensed layers of 1.0 10^{16} (curve A) and 2.0 10^{16} CO_2/cm^2 (curve B) and of H_2 on Cu plated stainless steel (curve C) at 4.2 K.

In the same way as for the CO and CH_4 condensates, two adsorption isotherms of H_2 on precondensed layers of CO_2 were measured. The adsorption isotherms of H_2 on a precondensed layer of 1.0 10^{16} CO_2/cm^2 and 2.0 10^{16} CO_2/cm^2 as well as the isotherm of H_2 on the clean Cu surface are shown in fig.3c. The H_2 adsorption capacity of CO_2 is considerably larger than that of CO or CH_4. For the case of a precondensed layer of 2.0 10^{16} CO_2/cm^2 the value of S where the steep pressure rise takes place is about 4 times larger than for the clean Cu surface. There is another distinct difference between precondensed CO_2 and CO (CH_4). When H_2 is injected into the system there is an immediate pressure rise in the system an effect which has not been seen when the surface was clean or covered with a condensate of CO or CH_4.

C. Co-adsorption of H_2 and CO, CH_4 and CO_2

The adsorption isotherm for co-adsorption of different mixtures of H_2 and CO plotted as a function of the S of H_2 are shown in fig.4a. The conditions were the same for all adsorption isotherms. In fig.4a it can be seen that the coadsorption does not have a significant effect on the value of S of H_2 at which the steep pressure rise starts, but it has a strong influence on the development of the pressure with increasing S. The isotherms were measured over a period of 5-8 h with the injection of a small amount of gas every 20 minutes and a reading of the pressure taken just before making a new gas injection.

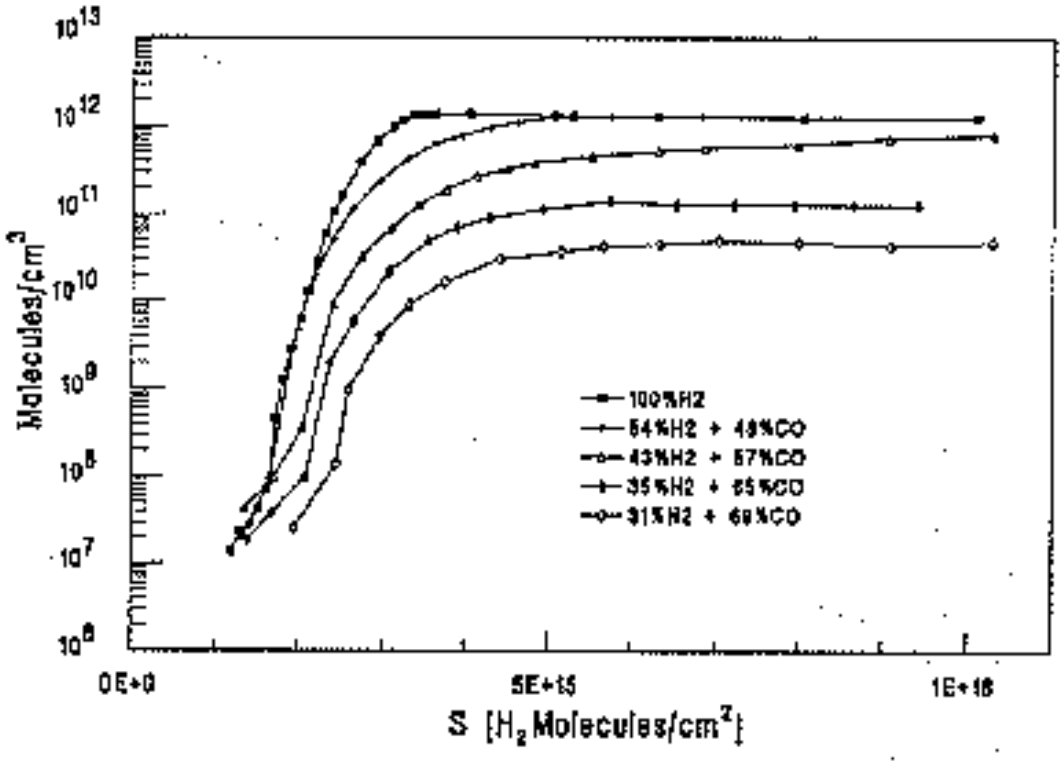

Fig.4a Isotherms of co-adsorption of H_2 and CO on Cu plated stainless steel at 4.2 K plotted as a function of the surface density of H_2 molecules.

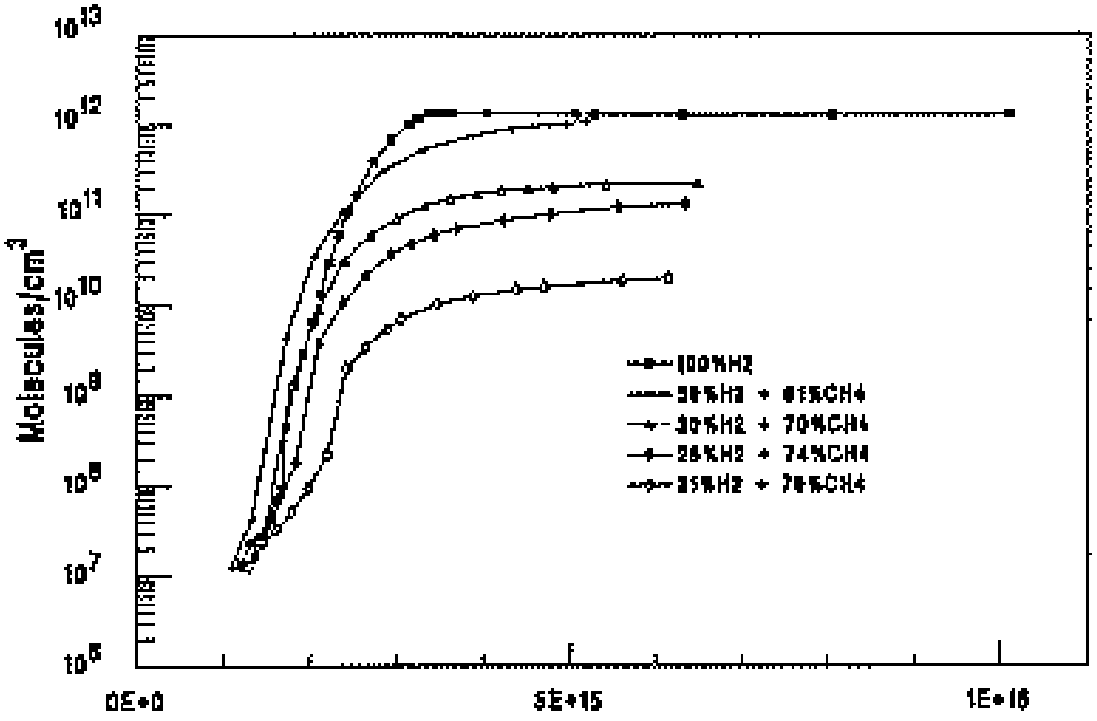

Fig.4b Isotherms of coadsorption of H_2 and CH_4 on Cu plated stainless steel at 4.2 K, plotted as a function of the surface density of H_2 molecules.

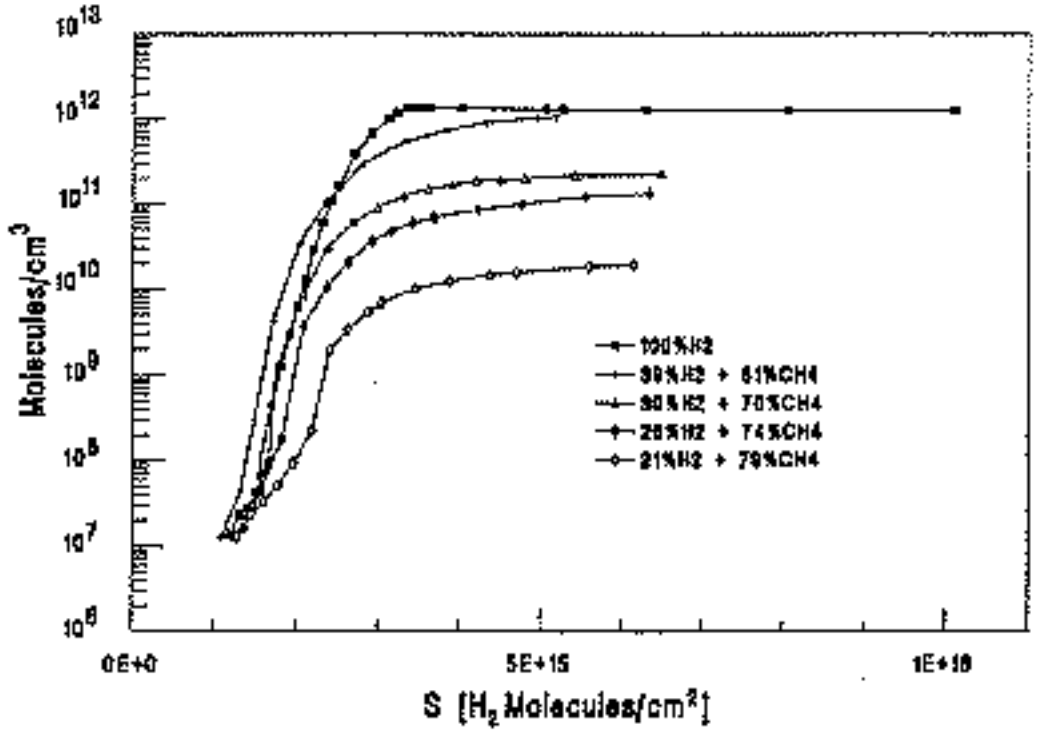

Fig.4c Isotherms of coadsorption of H_2 and CO_2 on Cu plated stainless steel at 4.2 K, plotted as a function of the surface density of H_2 molecules.

H_2 has been co-adsorbed with CH_4 following the same procedure as described above and the resulting isotherms plotted as a function of the S of H_2 are shown in fig.4b. In fig.4b we can see that CH_4 cryotraps H_2 less efficiently than CO. It seems as if the capacity at low coverage of the surface to adsorb H_2 has even decreased for the 39%H_2 + 61%CH_4 mixture compared to adsorption of pure H_2. The isotherms were measured under the same conditions as the H_2 + CO isotherms starting about 3h after the He fill of the cryostat and a total duration of the measurement between 5 and 8 h with about 20 minutes between each gas injection.

Coadsorption isotherms of mixtures of H_2 and CO_2 show that CO_2 is a more efficient gas for cryotrapping H_2 at 4.2 K than CO and CH_4. The measured adsorption isotherms for different mixtures of H_2 and CO_2, plotted as a function of the S of H_2 is shown in fig.4c. The conditions during the measurements were the same as for the co-adsorption isotherms reported above.

D. Simulation of the situation in the LHC

As mentioned earlier, the vacuum behaviour of the cold vacuum system of the LHC, as well as in most high energy accelerators, stems from synchrotron radiation induced desorption of gas from the metal walls of the vacuum chamber in the accelerator. With the assumption that the photodesorption process at 4.2 K is similar to the room temperature behaviour, we can expect to have about the same relation between the quantities of desorbed gases at 4.2 K as at room temperature.

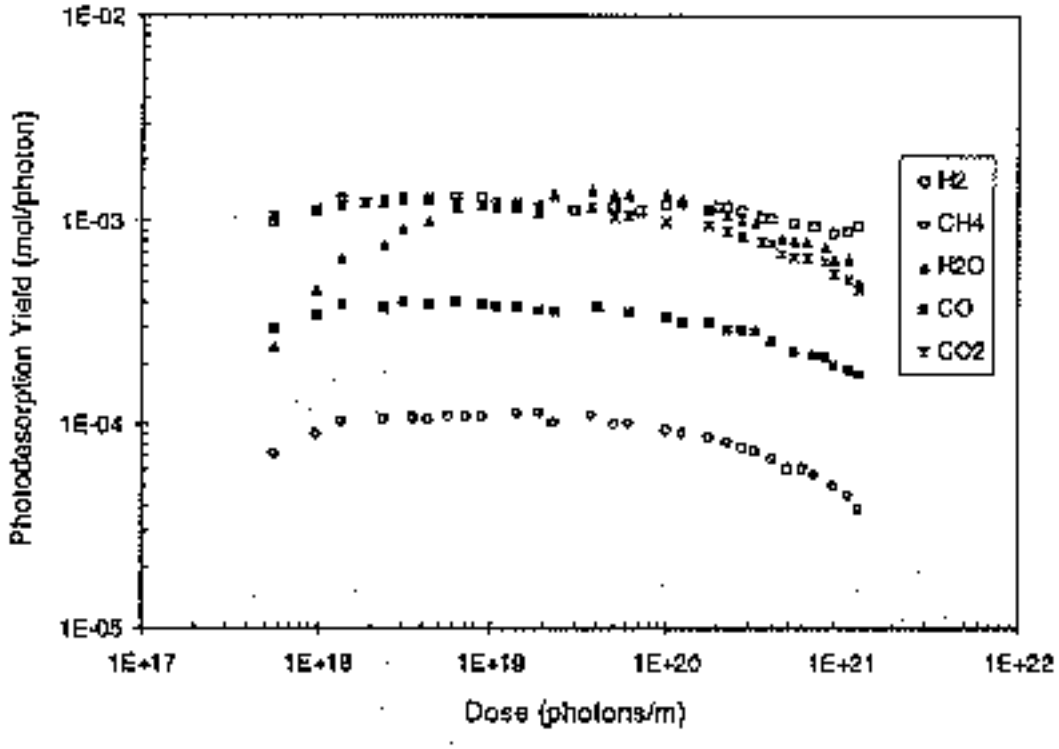

Fig.5 The photon induced gas desorption yields from an unbaked Cu plated stainless steel chamber at ambient temperature as a function of photon dose of synchrotron radiation with a critical energy of 63.5 eV, from ref.2

The desorption yields (molecules/photon) for unbaked Cu plated stainless steel at room temperature and a critical energy of the synchrotron radiation of 63.5 eV[2] are shown in fig.5. 63.5 eV is slightly higher than the critical energy in the LHC of 41.4 eV. The assumption that the ratio between the desorption yields for different desorbed gas species is not affected by the temperature difference between room temperature and 4.2 K is questionable[56,57], but it is a first approximation which so far has not been definitely ruled out.

From fig.5 we can see that the initial desorption yields for H_2 , CO_2, CO and CH_4 are equal to 1.2 10^{-3}, 1.2 10^{-3}, 3.0 10^{-4} and 1.0 10^{-4} mol/photon which would give a composition of the desorbed gas equal to 43%H_2, 43% CO_2, 10%CO and 4%CH_4. H_2O is neglected in this study since its desorption yield is varying and it is also difficult to use H_2O vapour in a UHV system, especially at low temperatures. The isotherm of coadsorption at 4.2 K of 43.0%H_2, 42.6% CO_2, 10.4%CO and 4.0%CH_4 has been measured and the isotherm is shown in fig.6, where it is plotted with the H_2 surface density on the x-axis and also compared to the H_2 isotherm on a clean surface. We can see that there is a significant suppression of the pressure compared to pure H_2 but there is no important effect on the H_2 coverage at which the pressure rise starts.

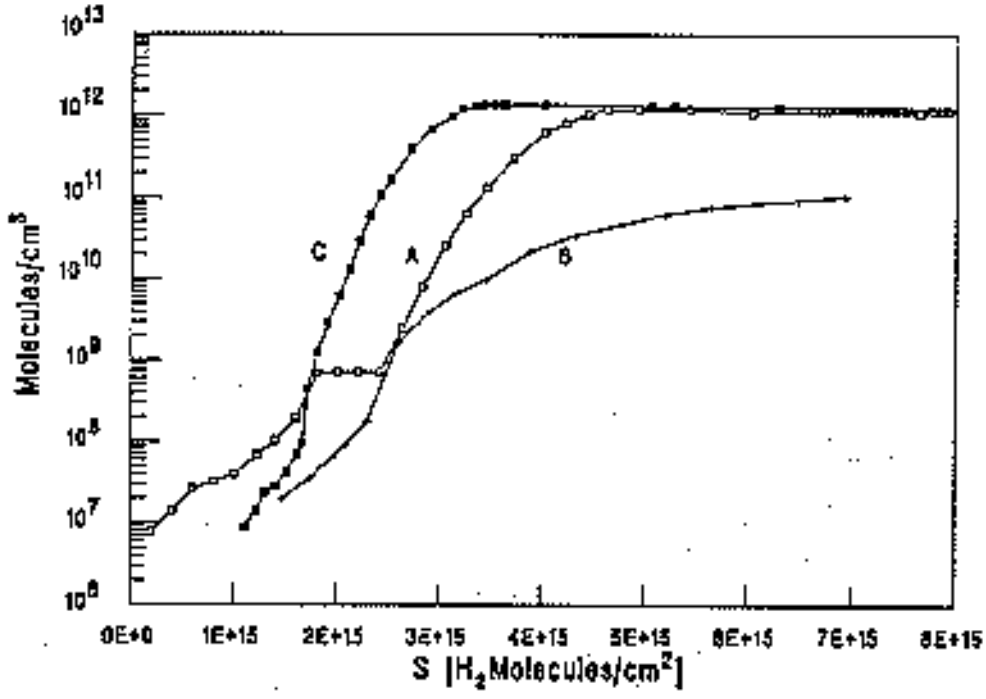

Fig.6 Isotherms of H_2 on a precondensed layer of 1.0 10^{16} molecules/cm^2 consisting of 74.0% CO_2, 18.8%CO and 7.2% CH_4 (curve A) and of coadsorption of 43.0% H_2, 4.0% CH_4, 10.4% CO and 42.6% CO_2 (curve B) on Cu plated stainless steel at 4.2 K, plotted with the H_2 surface density on the x-axis and of H_2 on Cu plated stainless steel at 4.2 K (curve C).

The adsorption isotherm for H_2 on a precondensate of CH_4, CO, and CO_2, mixed in about the same proportions as their desorption yields is shown in fig.6, together with the adsorption isotherm of H_2 on the clean surface. The condensate which consists of 74.0% CO_2+18.8%CO+7.2%CH_4, was injected into the system just after the He fill of the cryostat and about 3 h later the isotherm measurement started. The total number of molecules in the precondensed layer was 1.0 10^{16} molecules/cm^2. The large content of CO_2 in the precondensate gives the effect, as already seen for pure CO_2, at low H_2 coverage there is a measurable rise in pressure over the surface. There is a distinct plateau in the isotherm where it crosses the isotherm of the H_2 on the clean Cu. The reason for the plateau is not known.

E. He and Xe isotherms

The isotherms for He at 4.2 K and Xe at 77 K (liquid N_2) have been measured with exactly the same set-up as for the other measurements[60]. The high ratio of volume over the cold surface area in the present experimental set-up makes measurements for pressures higher than about 10^{-4} torr unreliable. This is unfortunate since roughness factor estimates by the BET method using the Xe adsorption isotherm would have been interesting. The two isotherms have been measured over a large pressure range and in fig.7 the isotherms of He at 4.2 K, Xe at 77 K and H_2 at 4.2 K are plotted.

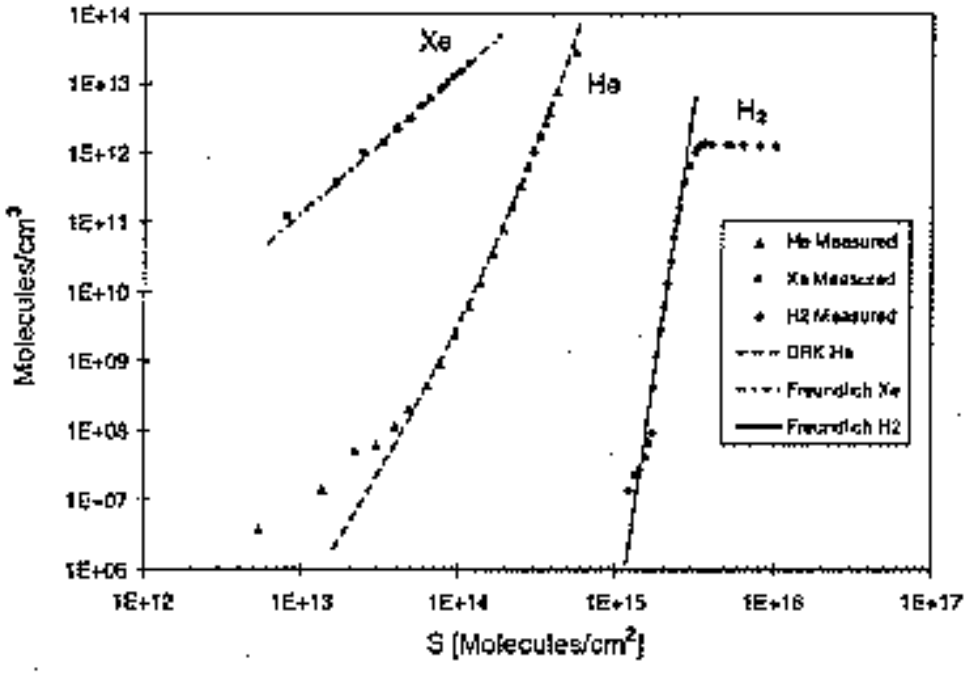

Fig.7 Isotherms of He and H_2 at 4.2 K and Xe at 77 K on Cu plated stainless steel. The following equations have been used in the plot: DRK He $S=1.84\cdot10^{15}\exp(-3.08\cdot10^{4}(kT\ln(n/n_0))^2)$, Freundlich H_2 $S=4.76\cdot10^{14}\cdot n^{1/15.6}$, Freundlich Xe $S=3.15\cdot10^{7}\cdot n^{1/2.03}$, where n represents the volume density, S the surface density and n_0 is the measured saturated vapour density of He at 4.2 K equal to 1.75 10^{21} He/cm^3.

IV. DISCUSSION

A. H_2 isotherm

The radical change in the shape of the isotherm at S = 1.65 10^{15} H_2/cm^2 and the later saturation at S = 3.3 10^{15} H_2/cm^2 lead to the conclusion that one monolayer consists of 1.65 10^{15} H_2/cm^2. There is a detectable pressure rise in the system only when the first monolayer approaches completion. As soon as the first layer of H_2 molecules is completed there is an immediate decrease in the adsorption energy. The effect of the lower adsorption energy is seen in the very steep pressure rise for S > 1.65 10^{15} H_2/cm^2. From the start of the third layer at S = 3.3 10^{15} H_2/cm^2 and onwards, there is no change in the adsorption energy with increasing thickness. The small pressure decrease of about 10% seen at S larger than 5 10^{15} H_2/cm^2 might be due to that the sticking coefficient increases somewhat compared to lower S as the H_2 condensate starts to form islands[16]. The heat of adsorption for solid H_2 is 8.5 meV[52] per molecule. It is not possible to give a quantitative value for the adsorption energy for S < 3.3 10^{15} H_2/cm^2. Such an estimate would assume the equality between the rate of adsorption and the rate of desorption at an equilibrium pressure. The rate of adsorption could be estimated with reasonable accuracy since the sticking coefficient σ for H_2 on Cu is known[10]. The rate of desorption, given by Frenkel's formula $\beta_0 \exp(-\Delta H_a/kT)$, which depends exponentially on the adsorption energy also has a pre-exponential evaporation coefficient β_0 which can vary more than a factor 10^3 for different values S of H_2 on Cu[52]. Hence it is not possible to say whether the variation of the rate of desorption with S depends on a variation in adsorption energy or a variation in the pre-exponential factor. Qualitatively the adsorption energy has to be higher for small S than for bulk H_2 since the pressure is lower than the saturated vapour pressure and hence the H_2 molecules are more strongly bound to the Cu surface than to solid H_2. There is a maximum value for the adsorption energy for the physisorption of H_2 on Cu of 25.5 meV[10]. On the other hand the sojourn time, i.e. the mean time which a molecule sits on the surface, can be estimated by simply dividing S by the rate of adsorption. The rate of adsorption for H_2 at 4.2 K is equal to σ 1.207 10^{22} P $H_2 s^{-1} cm^{-2}$ with P, the equlibrium pressure, in torr or σ 5.251 10^3 n $H_2 s^{-1} cm^{-2}$ where n is the equilibrium gas density in H_2/cm^3 and σ is the sticking coefficient. Based on ref.10 the author assumes the following behaviour of σ: at S = 0 H_2/cm^2 σ = 0.15 and σ increases linearly up to σ = 1 at the completion of the first monolayer, i.e. S = 1.65 10^{15} H_2/cm^2, and σ = 1 for all surface densities of H_2 exceeding one monolayer. The sticking coefficient for H_2 impigning on thick layers of condensed H_2 has been measured by, among others, Chubb and Pollard[58] and they found a value close to 1.

In fig.8 the measured isotherm for H_2 has been compared to the different isotherm equations described in Section I and the different isotherm equations fitted to the measured points have been plotted. It is obvious that Henry's law equation (2) is not valid for the measured isotherm since there is no linear correspondence between surface density and pressure. The Freundlich isotherm equation (3) describes the measured isotherm relatively well over a wide pressure range up to where the second monolayer starts to fill up. A plot according to the Freundlich equation (3)

has given the constants in equation (3) the values $c=7.12\cdot10^{15}$ and n=15.6. The Langmuir isotherm equation (4) describes the submonolayer part of the isotherm well with the constants in equation (4) put to $S_m=1.75\ 10^{15}\ H_2/cm^2$ and the constant $b = 3.95\ 10^{11}\ Torr^{-1}$. A BET plot has given the constants in equation (6) the values $S_m= 2.22\ 10^{15}\ H_2/cm^2$ and $\alpha = 7.86\ 10^3$. The BET equation (6) describes the isotherm reasonably well at higher pressures but it deviates considerably from the measured isotherm in the low pressure region. A DRK plot of the measured isotherm has given the constants in equation (10) the values $D = 3.61\ 10^4\ eV^{-2}$ and $S_m = 2.39\ 10^{15}\ H_2/cm^2$. The DRK equation (10) which in general describes the low pressure part of a physisorption isotherm quite well has in this case been shown not to reproduce the shape of the isotherm even though it is a reasonable fit to the measured isotherm over a large pressure range. The resulting adsorption isotherms, together with the estimated sojourn time for the molecules, are shown in fig.8. The author has found the Freundlich equation (3) to be the most appropriate isotherm equation to fit to the measured data points.

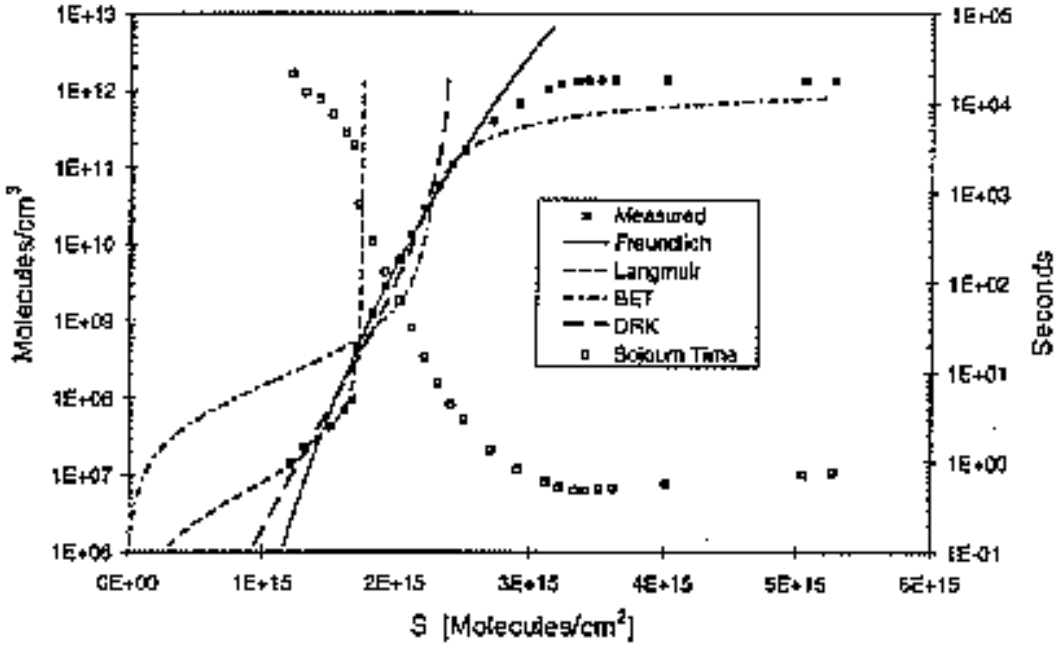

Fig.8. Fit of isotherm equations to the measured H_2 isotherm and a plot of the mean sojourn time for the adsorbed H_2 molecules at 4.2 K. The following equations have been used in the plot: Freundlich $S=4.76\cdot10^{14}\cdot n^{1/15.6}$, Langmuir $S=2.99\cdot10^{8}\cdot n/(1+1.72\cdot10^{-7}\cdot n)$, BET $S=5.74\cdot10^{-2}\cdot n/((n_0-n)(1+(7.86\cdot10^{3}-1)\cdot n/n_0))$, DRK $S=2.39\cdot10^{15}\exp(-3.61\cdot10^{4}(kT\ln(n/n_0))^2)$, where n represents the volume density, S the surface density and n_0 is the measured H_2 saturated vapour density at 4.2 K equal to $1.36\ 10^{12}\ H_2/cm^3$.

B. Adsorption of H_2 on gas condensates of CO, CH_4 and CO_2

The adsorption isotherms for H_2 on precondensed layers of CO and CH_4 containing $1\cdot10^{16}$ and $2\cdot10^{16}\ mol/cm^2$ show small deviations from the adsorption isotherm for H_2 on Cu-plated stainless steel. The adsorption capacity for a precondensed layers of $1\cdot10^{16}\ mol/cm^2$ of CO or CH_4 is a few percent smaller than for the Cu surface and if the layers contain $2\cdot10^{16}\ mol/cm^2$ the adsorption capacity has increased a few percent. This

might indicate that the surface of the CO or CH_4 condensate is smoother than the underlying Cu surface. The increase in adsorption capacity for thicker layers of precondensed CO or CH_4 may indicate that it is possible for H_2, to a small extent, to penetrate and get absorbed within the structure of the CO condensate.

When H_2 is adsorbed on precondensed CO_2 there are important differences compared to the isotherm of pure H_2 on Cu-plated stainless steel. When adsorbing H_2 on precondensed CO_2, there is an increase in pressure relative to the isotherm on the bare metal of about $3 \cdot 10^{-11}$ Torr corresponding to $7 \cdot 10^{7}$ H_2/cm^3 already at very low S of H_2. At intermediate values of S of H_2 the H_2 pressure is reduced below the bare metal isotherm and the adsorption capacity of CO_2 is large, much larger than for CO and CH_4. It seems like the interaction between H_2 and CO_2 is different from the other combinations. Schulze[39], who measured the adsorption of H_2 on a precondensed layer of $6 \cdot 10^{19}$ CO_2/cm^2 had a low pressure detection limit in his system of about 10^{-9} Torr which corresponds to $2 \cdot 10^{10}$ H_2/cm^3, did not, of course, see this effect at 4.2 K but there are no indications in the measurements from Schulze that there would be a H_2 pressure at low S over a CO_2 condensate exceeding his low pressure detection limit in the temperature region 4-22 K. Schulze also predicts a H_2 DRK monolayer capacity of a CO_2 condensate formed at 4.2 K to be about 0.073 ($molH_2/molCO_2$); considerably higher values have been obtained by others[59]. Tölle[25] measured the adsorption of H_2 on a precondensed layer of about 6 10^{19} CH_4/cm^2 and found, for a CH_4 condensate formed at 4.2 K, a DRK monolayer capacity for H_2 of about 0.040 ($molH_2/molCH_4$). Even though the present study considers much thinner layers where the adsorption capacity on the topmost surface of the condensate is comparable or even exceeding the adsorption capacity of the condensate, we can estimate the DRK monolayer capacities by looking at the difference between the two measured isotherms for each precondensed gas. If the measured isotherms for H_2 on the precondensed layers of $2.0 \cdot 10^{16}$ and $1.0 \cdot 10^{16}$ CO, CH_4 and CO_2 per cm^2 are plotted according to the DRK equation, the following DRK adsorption capacities for the condensate gases are found: CH_4 0.031 ($molH_2/molCH_4$), CO 0.043 ($molH_2/molCH_4$)and CO_2 0.31 ($molH_2/molCO_2$). The DRK equation does not reproduce the shape of the measured isotherms of H_2 on the different gas condensates in this study over a large range of surface densities of H_2, but it is a good approximation to the steepest part of the isotherms and also its definition of a monolayer makes it useful in the treatment of porous adsorbents and gas condensates. In addition it has shown to be an equation which can give good predictions of the temperature behaviour of physisorption isotherms on gas condensates[52,25,33,39]. The measured H_2 pressure at low surface concentrations of H_2 on the CO_2 condensates show that for porous adsorbents it is not possible to extrapolate the pressure given by the DRK equation down to infinitely low pressures.

C. Co-adsorption of H_2 and CO, CH_4 and CO_2

The measurements on the co-adsorption of H_2 and CO, H_2 and CH_4 and H_2 and CO_2 have shown that there is no essential difference in the shape of the H_2 isotherm during the co-adsorption of the different mixtures of the gases,

but the co-adsorption affects the value S at which the pressure rise is seen and the saturated vapour pressure which is obtained. The H_2 saturated vapour pressure at 4.2 K can be suppressed by orders of magnitude by the cryotrapping process and also the value S of H_2 where it is reached can be considerably larger than for adsorption of pure H_2. From the curves of co-adsorption of H_2 and CO, H_2 and CH_4 and H_2 and CO_2 in fig.4a, fig.4b and fig4c, it is seen that CO_2 is the most efficient gas in the cryotrapping process followed by CO and the least efficient gas is CH_4. The difference is surprisingly large considering that all three condensates have the same crystal structure and roughly the same nearest neighbour distance as solids, see section I.F. CH_4 does not have a strong effect on the value of S of H_2 for which the steep pressure rise starts and the mixture has to contain more than 60% of CH_4 before an effect on the H_2 saturated vapour pressure is seen. CO has a greater influence on the value S of H_2 at which the steep pressure rise takes and already at about 55% of CO in the mixture an effect on the H_2 saturated vapour pressure is seen. CO_2 is the most efficient gas to trap H_2 of the three and already at 45% of CO_2 in the gas mixture there is an effect on the saturated vapour pressure. The value of S of H_2 where the steep pressure rise is seen is also considerably higher for the CO_2 and H_2 mixture than for pure H_2. It has to be mentioned that the measured co-adsorption isotherms are representative for the time scale of the experiment, i.e. a few hours, and the long term behaviour of the mixed condensates is not treated in this study.

D. He and Xe isotherms

The measured adsorption isotherm for He at 4.2 K on Cu-plated stainless steel is well described by the DRK equation (10) while the Xe isotherm on the same surface at 77 K is well described by the Freundlich equation (3). In the low pressure part of the He isotherm, the measured points start to deviate from the DRK isotherm and approach the isotherm of Henry's law which predicts a linear relation between pressure and surface density of the adsorbate gas. It is in the intermediate region well below a complete monolayer that the DRK equation resembles the shape of the isotherm best and it seems to be the isotherm which takes over when Henry's law is no longer valid. The DRK plot of the measured isotherm for He at 4.2 gave the constants in (10) the values $D = 3.08\ 10^4\ eV^{-2}$ and $S_m = 1.84\ 10^{15}\ He/cm^2$ and for Xe at 77 K[60] the constants in (3) have the values $c = 8.63\ 10^{15}\ cm^{-2}$ and $n = 2.03$. The DRK fit to the He data together with the fit of the Freundlich equation (3) to H_2 at 4.2 K and Xe at 77 K are shown in fig.7.

V. CONCLUSIONS

One monolayer of H_2 on the Cu plated stainless steel surface consists of $1.65 \cdot 10^{15}$ H_2/cm^2 which, assuming closest packing and with a surface requirement per H_2 molecule[61] of $1.225\ 10^{-15}\ cm^2$, gives a ratio of real surface area over geometric surface area equal to 2.0. The saturated vapour pressure of H_2 at 4.2 K is reached at completion of the second monolayer which corresponds to a surface coverage of $3.3 \cdot 10^{15}$ H_2/cm^2 on the Cu plated stainless steel surface. The adsorption isotherm of H_2 on Cu plated stainless

steel at 4.2K has been compared to a number of adsorption istherm equations, described in section I.C, and the Freundlich equation (3) has shown to best resemble the isotherm.

A cryotrapping effect with a reduced saturated vapour pressure and capture of H_2 in the mixed condensate is seen when H_2 is co-adsorbed with CH_4, CO and CO_2. CO_2 has been found to be the most efficient gas of the three to cryotrap H_2 followed by CO and CH_4. A result which is in agreement with others[32,35,62].

Measurements of the adsorption isotherms of H_2 on precondensed layers of CO_2, CO and CH_4 show that the adsorption capacity of CO_2 is larger than the adsorption capacity for CO and CH_4. The DRK equation (10) is the isotherm which best describes the physisorption on gas condensates[24,25,38,39] and the DRK H_2 monolayer adsorption capacities for the different condensed gases were equal to: 0.031 ($molH_2/molCH_4$), 0.043 ($molH_2/molCO$)and 0.31 ($molH_2/molCO_2$). The values for CH_4 and CO_2 agree with measurements by others[25,40,59,63]. There is an increase in H_2 pressure of about $3{\cdot}10^{-9}$ Torr corresponding to $6{\cdot}10^{7}$ H_2/cm^3 already at very low surface densities of H_2 adsorbed on precondensed CO_2, an effect which not has been found when adsorbing H_2 on the Cu surface or precondensed CO and CH_4.

The isotherm of He on Cu plated stainless steel at 4.2 K is well described by the DRK equation (10) except at the low pressure end where the isotherm approaches Henry's law equation (2). The isotherm of Xe on Cu plated stainless steel at 77 K is described by the Freundlich equation (3).

VI. ACKNOWLEDGEMENTS

The author would like to thank Prof.S.Andersson and Dr.R.S.Calder for fruitful discussions, Dr.O.Gröbner and Dr.A.G.Mathewson for the possibility to make this study and Mr.J.M.Rieubland, Mr.G.Ferlin and the CERN Cryolab team for providing the experimental facilities and the precious liquid He. The author is also indebted to Mr.A.Grillot for valuable technical assistance in the conception and construction of the equipment.

VII. REFERENCES

[1] The Large Hadron Collider Accelerator Project, CERN/AC/95-05(LHC), 20 October 1995.

[2] B.Angerth, F.Bertillini, J.-C.Brunet, R.Calder,JGomez-Goni, O.Gröbner, A.Mathewson, A.Poncet, C.Reymermier, and E.Wallén, LHC Note 284, CERN/AT-VA/94-28, EPAC94, London, 26 June-1 July 1994.

[3] S.Andersson and J.Harris, Phys. Rev. Letters 48 (1982) 545.

[4] L.W.Bruch, Surface Science 125 (1983) 194-217.

[5] P.Nordlander, C.Holmberg and J.Harris, Surface Science 152/153 (1985) 702-709.

[6] P.Nordlander, C.Holmberg and J.Harris, Surface Science 175 (1986) L753-L758.

[7] E.Zaremba and W.Kohn, Phys. Rev. B 13 (1976) 2270

[8] L.Wilzén, Ph.D. Thesis, Chalmers University of Technology,Sweden (1989)

[9] G.Armand and J.R.Manson, Surface Science 119 (1982) L299-L306

[10] S.Andersson, J.Harris, M.Persson and L.Wilzén, Phys. Rev. B, Volume 40, Number 12 (1989) 8146.

[11] J.Perreau and J.Lapujoulade, Surface Science 122 (1982) 341-354.

[12] J.Perreau and J.Lapujoulade, Surface Science 119 (1982) L292-L298.

[13] S.Andersson, M.Persson and L.Wilzén, Physical Review B, Volume 38, Number 5 (1988) 2967.

[14] S.Andersson, J.Harris and L.Wilzén, Phys. Rev. Letters, Volume 55, Number 23 (1985) 2591

[15] S.Andersson, J.Harris and L.Wilzén, Surface Science 205 (1988) 387-396.

[16] Cryopumping, R.A.Haefer,Clarendon Press, Oxford (1989) p.72

[17] Proposed by William Henry (1803-1805)

[18] D.M.Young and A.D.Crowell, Physical Adsorption of Gases (1962), pp.104-106.

[19] H.Freundlich, Kapillarchemie, Leipzig,1930, Vol. I

[20] Scientific Foundations of Vacuum Technique, Saul Dushman,pp.385-389

[21] Scientific Foundations of Vacuum Technique, Saul Dushman,pp.390-394.

Original paper: I.Langmuir, J. Am. Chem. Soc, 40, 1361 (1918).

[22] J.P.Hobson, J. Chem. Physics 34 (1961) 1850.

[23] M.G.Kaganer, Dokl. Akad. Nauk. SSSR 138(1961) 405.

[24] K.E.Templemeyer, Cryogenics 11,120 (1971)

[25] V.Tölle, Ph.D. thesis, Technical University , Berlin (1971)

[26] Scientific Foundations of Vacuum Technique, Saul Dushman,pp.395-400,

Original paper: S.Brunauer, P.H.Emmett and E.Teller, J. Amer. Chem. Soc. 60 (1938) 309

[27] D.M.Young and A.D.Crowell, Physical Adsorption of Gases (1962), P.147-170.

[28] D.M.Young and A.D.Crowell, Physical Adsorption of Gases (1962), P.137-146,

Original Paper: M.Polanyi, Z.Elektrochem. 26,(1920) 371

[29] W.Sculze, Ph.D thesis, Technical University, Berlin (1971),

Original papers:M.M.Dubinin and L.V.Radushkevich, Proc.Acad.Sci.USSR 55 (1947) 327;

M.M.Dubinin, Russian J.Phys.Chem. 39 (1965) 487;

M.M.Dubinin, J.Coll.Int.Sci. 23 (1967) 487

[30] W.Sculze, Ph.D thesis, Technical University, Berlin (1971),

Original paper: M.G.Kaganer, Proc.Acad.Sci.USSR 116 (1957) 603;

[31] J.P.Hobson, J. Phys. Chem, 73 (1969) 2720

[32] Cryopumping, R.AHaefer,Clarendon Press, Oxford (1989) pp. 121-131.

[33] K.Wandelburg, , Ph.D thesis, Technical University, Berlin (1971).

[34] J.Hengevoss and E.A.Trendelburg , Vacuum, Vol. 17, No. 9 (1967) 495-500.

[35] B.Schimpke,K.Schugerl, Chemie-Ing.-Techn. 8 (1968) p. 392

[36] S.A.Stern, R.A.Hemstreet, and D.M.Ruttenbur, JVST. 3, 99 (1965)

[37] S.A.Stern, J.T.Mullhaupt, R.A.Hemstreet and F.S.Dipaolo, JVST. 2, 165 (1965)

[38] Cryopumping, R.AHaefer,Clarendon Press, Oxford (1989) pp. 85-106.

[39] W.Sculze, Ph.D thesis, Technical University, Berlin (1971),

[40] K.E.Templemeyer, R.dawbarn, and R.L.Young, JVST Vol.8, No.4 (1971) 575

[41] I.Arakawa and Y.Tuzi, JVST.A 4 (3), (May/June 1986) 293-296

[42] I.Arakawa, M.Kobayashi and Y.Tuzi, JVST. 16(2),(Mar./Apr. 1979) 738-740

[43] V.B.Yuferov and P.M.Kobzev, Sov. Phys. Tech. Phys. 14, 1261 (1970)

[44] O.Bostanjoglo, Z.Physik 187 (1965) 444

[45] V.B.Yuferov, R.F.Bulatova, P.M.Kobzev, and V.S. Kosan, Sov. Phys. Tech. Phys. 13, (1968) 238

[46] Cryopumping, R.AHaefer,Clarendon Press, Oxford (1989) P.97

[47] I.Arakawa, M.Kobayashi and Y.Tuzi, JVST. 16(2),(Mar./Apr. 1979) 738-740

[48] J.H. Colvoell, E.K. Gill, J.Chem. Physics 36 (1962) 2223

[49] T.Feldmann, J.Romanko, H.L.Welsh, Canad.J.Physics 33(1955)138

[50] H.Kapulla, W.Gläser, Phys. Letters 31A (1970) 158

[51] L.Vegard, Z.Phys. 61, 185(1930)

[52] T.J.Lee, JVST, Vol. 9, No. 1 (1971) 257-261

[53] C.Benvenuti, R.S.Calder and G.Passardi, JVST, Vol. 13, No. 6 (1976) 1172-1182

[54] The Physical Basis of Ultra High Vacuum, P.A.Readhead, J.P.Hobson , E.V.Kornelsen (1968) p.284

[55] T.Edmonds and J.P.Hobson, JVST Vol.2 ,182 (1965)

[56] W.Turner, private communication

[57] V.Baglin, private communication

[58] J.NChubb and I.E.Pollard, Vacuum/ Volume 15/ number 10, pp.465 (1965)

[59] Cryopumping, R.AHaefer,Clarendon Press, Oxford (1989) p.98

[60] The Xe sensitivity for the Bayert-Alpert gauge is not known. The given values are the values displayed on the instrument.

[61] Cryopumping, R.AHaefer,Clarendon Press, Oxford (1989)p.94

[62] Kryo-Vakuumtechnik, Grundlagen und Anwendungen, R.AHaefer, Springer Verlag, Berlin (1981) pp. 108-112

[63] K.E.Templemeyer, JVST Vol.8, No.4 (1971) 612